Author Manuscript

Author Manuscript

Author Manuscript

Author Manuscript

HHS Public Access

Author manuscript

Circ Res. Author manuscript; available in PMC 2018 March 05.

Published in final edited form as:

Circ Res. 2007 March 02; 100(4): 527–535. doi:10.1161/01.RES.0000259041.37059.8c.

Pinch1 Is Required for Normal Development of Cranial and Cardiac Neural Crest–Derived Structures

Xingqun Liang[*], **Yunfu Sun**[*], **Jurgen Schneider**, **Jian-Hua Ding**, **Hongqiang Cheng**, **Maoqing Ye**, **Shoumo Bhattacharya**, **Ann Rearden**, **Sylvia Evans**, and **Ju Chen**

Department of Medicine (X.L., Y.S., H.C., M.Y., X.E., J.C.), School of Pharmacology (Y.S., S.E.), Department of Cellular and Molecular Medicine, School of Medicine (J.-H.D.), Department of Pathology (A.R.), University of California at San Diego, La Jolla; and Department of Cardiovascular Medicine (J.S., S.B.), University of Oxford, UK

Abstract

Pinch1, an adaptor protein composed of 5 LIM domains, has been suggested to play an important role in multiple cellular processes. We found that Pinch1 is highly expressed in neural crest cells and their derivatives. To examine the requirement for Pinch1 in neural crest development, we generated neural crest conditional *Pinch1* knockout mice using the *Wnt1-Cre/loxP* system. Neural crest conditional *Pinch1* mutant embryos die perinatally from severe cardiovascular defects with an unusual aneurysmal common arterial trunk. *Pinch1* mutants also exhibit multiple deficiencies in cranial neural crest–derived structures. Fate mapping demonstrated that initial migration of neural crest cells to the pharyngeal arch region occurs normally in the mutant embryos. However, in the cardiac outflow tract of mutants, neural crest cells exhibited hyperplasia and failed to differentiate into smooth muscle. Markedly increased apoptosis is observed in outflow tract cushions of mutants between embryonic days 11.5 and 13.5, likely contributing to the observed defects in cushion/valve remodeling and ventricular septation. Expression of transforming growth factor-β_2, which plays a crucial role in outflow tract development, was decreased or absent in the outflow tract of the mutants. The decrease in transforming growth factor-β_2 expression preceded neural crest cell death. Together, our results demonstrate that Pinch1 plays an essential role in neural crest development, perhaps in part through transforming growth factor-β signaling.

Keywords

Pinch1; mouse; neural crest cell; cardiovascular/craniofacial defects

Neural crest cells (NCCs) are a multipotent migratory cell population that emerges from the dorsal part of the neural tube to populate numerous structures along the dorsoventral axis.[1] Cranial NCCs arise from the forebrain and hindbrain region to populate craniofacial structures as well as pharyngeal arches 1 to 2, giving rise to cranial ganglia, the maxilla, the

Correspondence to Ju Chen, Department of Medicine, UCSD, School of Medicine, 9500 Gilman Dr, La Jolla, CA 92093-0613. juchen@ucsd.edu.

[*]Both authors contributed equally to this work.

Disclosures

None.

Author Manuscript Author Manuscript Author Manuscript Author Manuscript

mandible, and other structures of the head and neck.[2,3] Cardiac NCCs delaminate from rhombomeres 6, 7, and 8 of the postotic neural tube[2–4] and migrate lateroventrally into pharyngeal arches 3, 4, and 6.[5,6] Some cardiac NCCs contribute to the patterning of pharyngeal arch arteries, whereas others migrate further into the cardiac outflow tract, where they join together into ridges of the mesenchyme, giving rise to the spiral septum between the ascending aorta and the main pulmonary artery.[2,3,6,7] A subset of cardiac NCCs contributes to the smooth muscle component of the outflow tract.[8] A subpopulation of cardiac NCCs invades the outflow tract cushion, which will develop into the aortic and pulmonary valves.[8] In the endocardial cushions, cardiac NCCs may participate in inductive interactions with cushion mesenchyme. Perturbation of cardiac NCC development cause congenital heart defects in animal models and in humans, affecting the outflow tract and great vessels.[7,9–12]

Recently, tissue interactions and molecular mechanisms required for cardiac NCC development have been extensively studied. A growing list of genes has been shown to play a role in NCC formation, maintenance, migration, and differentiation, including members of the transforming growth factor-β (TGFβ) superfamily and their receptors.[1,13–15] TGFβ_2 is essential for outflow tract development,[16] and TGFβR2 is essential for differentiation of NCCs into smooth muscle and NCC-specific TGFβR2 knockout mice exhibit outflow tract remodeling defects.[14,17]

Pinch1, which is composed of 5 LIM domains arrayed in tandem, has been suggested to play an important role in processes as diverse as cell adhesion, migration, proliferation, differentiation, and survival.[18] Genetic studies in various species point to an essential role of Pinch1 in mediating integrin/integrin-linked-kinase (ILK)-dependent signaling.[19–21] Global *Pinch1* mutant embryos exhibit a disorganized egg cylinder with decreased cell proliferation and excessive cell death at embryonic day 5.5 (E5.5) and die at approximately E6.5,[21] similar to those of *ILK* and β_1-integrin knockout mice. Pinch1 also contains a presumed leucine-rich nuclear export signal and a basic nuclear localization signal, suggesting that it may act as a shuttling/signaling protein or function in transcription.[22]

In this study, we observed that Pinch1 is highly expressed in NCCs, in which it is mainly localized to the nucleus. To dissect its role in NCCs, we generated mice homozygous for a floxed allele of *Pinch1* and crossed these mice with *Wnt1-Cre* mice.[23] The resulting *Wnt1-Cre;Pinch1* mutant embryos display severe cardiovascular defects, including an unusual aneurysmal common arterial trunk, ventricular septal defects (VSDs) and defective cushion/valve maturation. These defects lead to perinatal death. Mutants also exhibit enlarged hearts with a thin right ventricular myocardium compact zone. In addition to cardiovascular defects, mutants exhibit hypoplastic glossopharyngeal ganglia (IX cranial ganglia), hypoplastic thymus, and malformations of bones and cartilage of the face, basal skull, and neck. Our data suggest that Pinch1 plays a crucial role in neural crest development.

Author Manuscript Author Manuscript Author Manuscript Author Manuscript

Materials and Methods

In Situ Hybridization

Whole-mount in situ hybridization was performed with digoxigenin-labeled RNA probes as previously described.[21]

Generation of Gene-Targeted Mouse Lines

The *Pinch1* targeting vector was constructed as previously described.[21] To generate *Pinch1* neural crest conditional knockout mice, mice homozygous for the *Pinch1* floxed allele were mated with *Wnt1-Cre* mice to generate mice with *Wnt1-Cre* and *Pinch1* heterozygous floxed alleles. *Wnt1-Cre;Pinch1* mutant mice were generated by backcrossing these mice to mice homozygous for the *Pinch1* floxed allele. For in vivo fate mapping of NCCs, *Wnt1-Cre* mice heterozygous for the *Pinch1* floxed allele were mated with animals homozygous for the *Pinch1* floxed allele carrying a *ROSA26 Lacz* reporter (*R26R*) allele,[24] which expresses β-galactosidase (β-Gal) on *Cre*-mediated recombination. Genotyping was performed as described[21] with the following primers: floxed Pinch1, forward 5′-CCCAGAAGGACTCTTTTATGAG-3′, and reverse, 5′-CTTGGAGAAGAAGTACTCAGGT-3′; Wnt1-Cre, forward, 5′-CCGGGCTGCCACGACCAA-3′, and reverse, 5′-GGCGCGGCAACACCATTTTT-3′. All the experiments involving mice were carried out according to a protocol reviewed and approved by the Institutional Animal Care and Use Committee of USCD, in compliance with the USA Public Health Service Policy on Humane Care and Use of Laboratory Animals.

Embryo Dissection and Histological Analysis

Females with copulation plugs were considered to be at embryonic development day 0.5 (E0.5) of gestation. Pregnant females were euthanized at different stages of gestation, and embryos were dissected for histological analysis as described.[21]

β-Gal Staining

Embryos presumably expressing β-Gal were harvested in cold PBS and fixed for 1 to 2 hours in 4% paraformaldehyde. To optimize tissue fixation and penetrance of β-Gal substrate (Roche Molecular, Indianapolis, Ind), the chest wall was opened before fixation and in some cases the heart was dissected and incubated in substrate. Both embryos and hearts were incubated in β-Gal substrate. For high-resolution analysis of β-Gal activity, embryos were paraffin embedded, sectioned, and counterstained with nuclear fast red.

Skeletal Preparations

Skeletal preparations of embryos were performed as described.[25] Briefly, cartilage was stained for 2 days in Alcian blue solution (150 mg/L Alcian Blue 8GX in 80% ethanol/20% acetic acid), and bones were stained with Alizarin red (50 mg/L Alizarin red S in 0.5% KOH) for several hours to overnight temperature. Clearing was performed using 0.25% KOH until soft tissues became transparent for photographs.

Author Manuscript Author Manuscript Author Manuscript Author Manuscript

Immunostaining

Immunostaining was performed as described.[21] Briefly, 5-μm sections were incubated with primary antibodies overnight at 4°C. The following primary antibodies were used: Pinch1[26]; ILK (1:550; Sigma, I0783); TGFβ_2 (1:400; Abcam, ab15539); p27 (1;200; Abcam, ab7961); α-smooth muscle actin (1:500; Abcam, ab7817); and P-Smad2 (1:200; Abcam, ab5478). After washing with 0.25% TritonX-100 in PBS, sections were incubated with either fluorescently labeled (Molecular Probes, Invitrogen, California, Calif) or biotinylated secondary (Vector) antibodies for 2 hours.

5-Bromodeoxyuridine Labeling and Apoptosis Assays

5-Bromodeoxyuridine (BrdUrd) labeling and apoptosis assays were performed as described.[21]

Neural Crest Cultures

We performed neural crest cell cultures as described.[27] Briefly, embryos were collected at E8.5 (4 to 10 somites), and the yolk sac from each embryo was harvested for genotyping by PCR analysis. Each embryo was treated with 0.5 mg/mL collagenase/dispase and then bisected longitudinally to expose the hindbrain neural folds. The portion of neural tube between the otic placode and the third somite was transected and cultured in a 35-mm fibronectin-coated Petri dish containing high-glucose DME and 10% fetal bovine serum. Cultures were maintained for 72 hours at 37°C with 5% CO_2, and then each neural tube explant was removed and discarded. Neural crest cell outgrowths attached to the culture for analysis.

MRI and Corrosion Casts

Embryos were analyzed by MRI as previously described.[28] Briefly, paraformaldehyde-fixed embryos were embedded in a MRI contrast agent and imaged using an 11.7 Tesla magnet. The 3D MRI dataset obtained was reconstructed into axial tagged image file format slices. Image datasets were analyzed and 3D reconstructions created using Amira 3.0 software. Corrosion casts were prepared and processed according to protocols in Baston's No. 17 Plastic Replica and Corrosion Kit (Polysciences Inc; catalog no. 07349).

Results

Pinch1 Is Highly Expressed in Premigratory and Migratory Neural Crest Cells

We examined Pinch1 expression in mouse embryos between E8.5 and E11.5 using whole-mount in situ hybridization and immunostaining. In situ hybridization analysis demonstrated that wide expression of Pinch1 in many tissues at various levels. At E8.5, Pinch1 was highly expressed in cranial neural folds (Figure 1Aa) and continued to be expressed in regions of migrating cranial and cardiac NCCs at E9.5 (Figure 1Ab). Immunohistochemical analysis in combination with *R26R* embryos[3] demonstrated prominent Pinch1 expression in NCC-derived structures, including outflow tract mesenchyme at E10.5 (Figure 1Bc and 1Bd) and outflow tract cushions at E11.5 (Figure 1Be through 1Bg). Biochemical and genetic studies have pointed to an essential role of Pinch1 as an adaptor protein in mediating ILK-dependent

Author Manuscript Author Manuscript Author Manuscript Author Manuscript

function.[19–21] We therefore analyzed the subcellular localization of Pinch1 and ILK in isolated NCCs. ILK was expressed in the cytoplasm (Figure 1C), whereas Pinch1 was primary expressed in the nucleus (Figure 1C), suggesting that Pinch1 in NCCs might play a role in the nucleus that is independent of its interaction with ILK.

Inactivation of *Pinch1* in the Neural Crest

Given its expression pattern, we investigated the potential role of Pinch1 in neural crest development. For this purpose, we used mice with a floxed allele of *Pinch1*,[21] enabling tissue-specific gene inactivation in the neural crest in *Wnt1-Cre* mice.[29] Thus, to generate neural crest–specific *Pinch1* mutants, mice heterozygous for the *Wnt1-Cre;Pinch1* floxed allele were crossed with homozygous floxed *Pinch1* mice. In *Pinch1* mutant embryos derived from the cross, Pinch1 expression was efficiently eliminated in all neural crest derivatives as determined by immunostaining with a Pinch1 specific antibody (Figure 1Bh). In contrast, littermates lacking the *Wnt1-Cre* transgene or carrying 1 wild-type *Pinch1* allele expressed Pinch1 normally and served as controls for our studies. To ensure that lack of Pinch1 expression in NCCs was not attributable to absence of the NCCs, we performed fate-mapping study in the neural crest–specific *Pinch1* mutants. As shown in Figure 1Bi, the NCCs are present in the mutant outflow tract.

Lethality and Cardiovascular Malformations in *Pinch1* mutants

All *Wnt1-Cre;Pinch1* homozygous mutants died perinatally. At E10.5, mutant embryos exhibited no obvious malformations (data not shown). However, from E13.5 to E18.5, mutants could be recognized by shortened mandibles and abnormal accumulation of blood within the cranial region (data not shown). Histological analysis revealed normal anatomy in littermate controls at E13.5 (Figure 2A through 2C) and E18.5 (Figure 3Aa through 3Ac), whereas all mutants exhibited complete failure of outflow tract septation, or persistent truncus arteriosus with an absence of a well-defined aorta and pulmonary trunk (Figure 2D through 2F; Figure 3Ad through 3Af). The single outflow tract in mutant embryos became progressively dilated from E11.5 onwards. In addition, VSDs, defective cushion-valve maturation, and enlarged hearts with a thin right-ventricular myocardium compact zone were observed in mutants between E16.5 and E18.5 (Figure 3Ad through 3Af). In agreement with histological analysis, MRI and 3D reconstruction revealed normal anatomy of E18.5 wild-type embryos (Figure 3Ba and 3Bb), whereas mutant embryos exhibited severe cardiovascular defects (Figure 3Bc and 3Bd), including VSDs and a right ventricular outflow tract, giving rise to a common arterial trunk (CAT), which was grossly dilated and formed an aneurysmal sac. In addition, corrosion casts showed that subclavian, common carotid, and pulmonary arteries, although abnormally patterned, were present in the mutant, all arising from the CAT (Figure 3C).

Defective Development of Cranial Neural Crest Derivatives

Hypoplastic thymus, smaller or absent glossopharyngeal ganglia, and disrupted submandibular glands were detected in *Pinch1* mutants at E13.5 (Figure 4B, 4D, and 4F) when compared with wild-type littermates (Figure 4A, 4C, and 4E). At E17.5 to 18.5, additional craniofacial anomalies were visible in mutants, including cleft palate (Figure 5B) and hypoplastic or malformed structures of bone and cartilage in the head and neck (Figure

Author Manuscript Author Manuscript Author Manuscript Author Manuscript

5D, 5F, 5H, and 5J) compared with control littermates (Figure 5A, 5C, 5E, 5G, and 5I). In mutants, the maxilla was incomplete or malformed and the mandible was smaller (Figure 5D and 5F). The base of the skull bone was also affected: orbitosphenoid, presphenoid, and basisphenoid bones were reduced in size (Figure 5D and 5F). In the developing ear, the otic capsule appeared normal, but the malleus and gonial bones were smaller (Figure 5H). In the neck region, the hyoid bone and thyroid cartilage were hypoplastic or malformed (Figure 5J). We did not observe obvious abnormalities in the calvarial bone, thyroids, and parathyroids of the mutants (data not shown).

NCC Migration and Distribution

To examine the migration and distribution of NCCs in *Pinch1* mutants we used fate mapping. For this purpose, we crossed *Wnt1-Cre;Pinch1* heterozygotes with mice homozygous for the *Pinch1* floxed allele and carrying an *R26R* reporter allele,[24] enabling us to visualize NCCs by β-Gal expression. At E9.5, *Pinch1* deficient NCCs were observed in a normal distribution in the cranial region, pharyngeal arches, and trunk region as compared with that of controls (Figure 6A and 6B), as indicated by β-Gal activity in whole-mount preparations. To further analyze cardiac NCC migration, we examined sections of embryonic tissue taken through the conotruncal region. At E10.5, NCCs, marked by β-Gal activity, were observed in the cranial region and pharyngeal arches as well as in the lateral walls of the aortic sac and truncus in a similar pattern in both mutants (Figure 6F through 6H) and control littermates (Figure 6C through 6E). Similar results were obtained by whole-mount in situ hybridization using a riboprobe for the neural crest marker *CrbpI* (Figure 6I and 6J). These results indicated that the initial migration of *Pinch1*-deficient NCCs was following the expected pattern and timing. However, from E11.5, an abnormal distribution of cardiac NCCs the outflow tract was observed in mutants. An increased number of NCCs was seen in the truncus of mutants (Figure 6M and 6P) relative to control littermates (Figure 6K and 6O), whereas a significantly reduced number of NCCs was observed in mutant outflow tract cushions/valves (Figure 6N and 6P) compared with control littermates (Figure 6L and 6O). Overall, these results demonstrated that the initial migration of NCCs into the pharyngeal arch and cardiac region occurs normally in mutant embryos.

Cell Death, Proliferation, and Differentiation Are Abnormal in *Pinch1* Mutants

Following analysis of NCC migration, we next examined cell death, proliferation, and differentiation in *Wnt1-Cre;Pinch1* mutants and littermate controls to further investigate events underlying the observed defects. For cell death analysis, TUNEL staining was performed on sections from E10.5 and E13.5 embryos. No significant cell death was detected in the outflow tract regions of both mutant and control embryos at E10.5 (data not shown). By E11.5, a few TUNEL-positive cells were observed in outflow tract cushions of control embryos (Figure 7A through 7C), whereas none was observed in the membranous septum of control embryos at E13.5 (Figure 7G through 7I). In contrast, mutant embryos exhibited markedly increased (≈8-fold) apoptosis in outflow tract cushions at E11.5 (Figure 7D through 7F). Apoptosis was also evident in the membranous septum of mutants at E13.5 (Figure 7J through 7L), whereas no apoptosis was observed in control embryos. Compared with the fate-mapping analysis in the adjacent section (Figure 7C, 7F, and 7L), apoptotic cells were mostly cardiac NCC-derived cells. Cell proliferation assays using BrdUrd

Author Manuscript Author Manuscript Author Manuscript Author Manuscript

labeling revealed increased BrdUrd incorporation in the outflow tract of mutants at E13.5 (Figure 7N) compared with controls (Figure 7M). Contribution of cardiac NCCs to smooth muscle differentiation was assessed by immunostaining with antibodies to p27 and α-smooth muscle actin (α-SMA), which mark postmitotic cells and differentiating smooth muscle cells, respectively. Cells in the outflow tract positive for both p27 and α-SMA were greatly reduced or absent in mutants (Figure 7P, 7S, and 7T) at E11.5 as compared with control littermates (Figure 7O, 7Q, and 7R). In contrast, the expression of α-SMA in mutants was normal in the pharyngeal arch artery and out layer smooth muscle cells of the outflow tract (Figure 7S), which arise from non neural crest cell lineages.

Potential Downstream Targets of Pinch1

Differentiation of cardiac NCCs to smooth muscle cells in the cardiac outflow tract was altered in mice with neural crest specific ablation of TGFÂR2.[14] Because cardiac NCC differentiation was affected in *Wnt1-Cre;Pinch1* mutants, we asked whether TGFβ signaling was altered in mutants by examining expression of TGFβ ligands. In situ hybridization (Figure 8A and 8B) and immunostaining (Figure 8C and 8D) demonstrated that expression of TGFβ_2 mRNA and protein was significantly downregulated or undetectable in the outflow tract and outflow tract cushions of mutants. This finding was further supported by the concomitant reduction of TGFβ-dependent phosphorylation of Smad2 in mutants (Figure 8F) as compared with control embryos (Figure 8E). Downregulation of TGFβ_2 expression in mutants was becoming evident at E10.5, a stage at which no significant apoptosis was detected, and became more evident by E11.5 as compared with control littermates (data not shown). These findings indicate that Pinch1 is required for TGFβ_2 expression.

Discussion

Our previous study revealed that mice with a conventional knockout of *Pinch1* died at early gastrulation,[21] precluding study of its role in later developmental stages. Here we showed that Pinch1 is widely expressed in embryos with the highest level of expression in NCCs. Therefore, we used a floxed allele of *Pinch1* and ablated *Pinch1* in the neural crest by *Cre* recombination driven by the *Wnt1* promoter. Mutant embryos died perinatally from severe cardiovascular defects, including persistent truncus arteriosus, aortic–pulmonary trunk anomalies, VSD, and enlarged heart with a thin ventricular myocardium compact zone, and hypoplasia of the thymus, which resemble phenotypes resulting from cardiac NCC ablation in chick.[2] However, mutant embryos also exhibited an unusual aneurysmal common arterial trunk and a significant increase in the number of NCCs in the region, which has not been observed in other mutant models.

Pinch1-deficient NCCs migrated correctly into the pharyngeal apparatus as demonstrated by in vivo fate mapping using *Wnt1-Cre;R26R* indicator mice and by in situ hybridization using the neural crest marker *CrbpI*. However, abnormal behavior of NCCs was observed in the outflow tract of mutants with a significant increase in the number of NCCs in the truncal region from E11.5 onward and a reduction in the number of NCCs in the outflow cushion from E13.5. Importantly, we found that E11.5 mutant cardiac NCCs in the outflow tract did not express p27, indicating their failure to exit the cell cycle, and also did not express α

Author Manuscript Author Manuscript Author Manuscript Author Manuscript

smooth-muscle-actin, a marker of smooth muscle cell differentiation. In addition, increased proliferation was observed in the outflow tract from E11.5 onwards. Together, these observations suggest that ablation of *Pinch1* in NCCs prevents their exit from the cell cycle and differentiation into smooth muscle cells. The lack of NCC differentiation might affect the elasticity of the outflow tract wall and result in an unusual aneurysmal common arterial trunk, whereas increased proliferation may lead to progressive thickness of the outflow tract wall.

Pinch1-deficient NCCs in the outflow tract cushion underwent markedly increased apoptosis at E11.5 to E13.5, associated with an observed failure of cushion remodeling and valve maturation. These observations demonstrate a requirement for *Pinch1* in survival of NCCs within outflow tract cushions.

Biochemical and genetic studies have provided compelling evidence that Pinch functions as an essential component of integrin/ILK signaling pathway.[19–21] Pinch1 and ILK form a tight complex that serves as a hub in the integrin–actin network through direct interaction of ILK with the cytoplasmic domain of integrin β_1[18] Integrins are transmembrane receptors that interact with the extracellular matrix and are required for cell migration, proliferation, differentiation, and apoptosis. However, deletion of β_1 integrin in NCCs does not cause defects in cardiac and cranial NCC-derived structures as observed here.[30] It is possible that other β integrins may compensate for the loss of integrin β_1, because it has been shown that ILK may also interact with integrin β_3 and/or β_5. We found no significant difference in the expression of ILK, fibronectin, and laminin in cultured NCCs and in the outflow tract of *Wnt1-Cre;Pinch1* mutants (data not shown), suggesting that inactivation of *Pinch1* in NCCs did not affect formation of the focal adhesion complex. In addition to its demonstrated role in the integrin–ILK–PINCH complex, Pinch1 contains a presumed leucine-rich nuclear export signal and an overlapping basic nuclear localization signal, suggesting that it may act as a shuttling/signaling protein or function in transcription.[22] Our finding that Pinch1 is present in the nucleus of NCCs is consistent with this idea and suggests the intriguing possibility that Pinch1 may be required in the nucleus within NCCs.

TGFβ signaling plays an important role in specification, migration, survival, and differentiation of NCCs.[1,14,31] We report here that specific deletion of Pinch1 in NCCs down-regulates TGFβ signaling and decreases Smad phosphorylation and that mutant mice display an aneurysmal common arterial trunk in addition to defective development of cranial NCC derivatives such as palate, thymus, craniofacial skeleton, and cranial ganglia. Our results suggest that aspects of the *Wnt1-Cre;Pinch1* mutant phenotype may result from decreased TGFβ signaling.

A unique feature of the neural crest Pinch1 mutant is, however, the aneurysmal arterial trunk. It is important to note that several human syndromes that include aortic and vascular aneurysms have been associated with alterations in TGFβ signaling.[32–34] These results lead us to speculate that Pinch1 mutation may be involved in human syndromes characterized by aortic and vascular aneurysms.

Author Manuscript Author Manuscript Author Manuscript Author Manuscript

Acknowledgments

Knockout mice were generated at the transgenic core facility at University of California at San Diego. We thank Drs Henry Sucov, Marie-Louise Bang, and Paul Grossfeld for critical reading of the manuscript.

Sources of Funding

The work was supported by the NIH (to J.C. and S.E.).

References

1. Le Douarin NM, Dupin E. Multipotentiality of the neural crest. Curr Opin Genet Dev. 2003; 13:529–536. [PubMed: 14550420]
2. Kirby ML, Waldo KL. Neural crest and cardiovascular patterning. Circ Res. 1995; 77:211–215. [PubMed: 7614707]
3. Jiang X, Rowitch DH, Soriano P, McMahon AP, Sucov HM. Fate of the mammalian cardiac neural crest. Development. 2000; 127:1607–1616. [PubMed: 10725237]
4. Kirby ML, Gale TF, Stewart DE. Neural crest cells contribute to normal aorticopulmonary septation. Science. 1983; 220:1059–1061. [PubMed: 6844926]
5. Miyagawa-Tomita S, Waldo K, Tomita H, Kirby ML. Temporospatial study of the migration and distribution of cardiac neural crest in quail-chick chimeras. Am J Anat. 1991; 192:79–88. [PubMed: 1750383]
6. Epstein JA, Li J, Lang D, Chen F, Brown CB, Jin F, Lu MM, Thomas M, Liu E, Wessels A, Lo CW. Migration of cardiac neural crest cells in Splotch embryos. Development. 2000; 127:1869–1878. [PubMed: 10751175]
7. Conway SJ, Henderson DJ, Copp AJ. Pax3 is required for cardiac neural crest migration in the mouse: evidence from the splotch (Sp2H) mutant. Development. 1997; 124:505–514. [PubMed: 9053326]
8. Brand T. Heart development: molecular insights into cardiac specification and early morphogenesis. Dev Biol. 2003; 258:1–19. [PubMed: 12781678]
9. Lipson AH, Yuille D, Angel M, Thompson PG, Vandervoord JG, Beckenham EJ. Velocardiofacial (Shprintzen) syndrome: an important syndrome for the dysmorphologist to recognise. J Med Genet. 1991; 28:596–604. [PubMed: 1956057]
10. Brannan CI, Perkins AS, Vogel KS, Ratner N, Nordlund ML, Reid SW, Buchberg AM, Jenkins NA, Parada LF, Copeland NG. Targeted disruption of the neurofibromatosis type-1 gene leads to developmental abnormalities in heart and various neural crest-derived tissues. Genes Dev. 1994; 8:1019–1029. [PubMed: 7926784]
11. Brown CB, Boyer AS, Runyan RB, Barnett JV. Requirement of type III TGF-beta receptor for endocardial cell transformation in the heart. Science. 1999; 283:2080–2082. [PubMed: 10092230]
12. Stoller JZ, Epstein JA. Identification of a novel nuclear localization signal in Tbx1 that is deleted in DiGeorge syndrome patients harboring the 1223delC mutation. Hum Mol Genet. 2005; 14:885–892. [PubMed: 15703190]
13. Stoller JZ, Epstein JA. Cardiac neural crest. Semin Cell Dev Biol. 2005; 16:704–715. [PubMed: 16054405]
14. Wurdak H, Ittner LM, Lang KS, Leveen P, Suter U, Fischer JA, Karlsson S, Born W, Sommer L. Inactivation of TGFbeta signaling in neural crest stem cells leads to multiple defects reminiscent of DiGeorge syndrome. Genes Dev. 2005; 19:530–535. [PubMed: 15741317]
15. Lindsay EA, Vitelli F, Su H, Morishima M, Huynh T, Pramparo T, Jurecic V, Ogunrinu G, Sutherland HF, Scambler PJ, Bradley A, Baldini A. Tbx1 haploinsufficieny in the DiGeorge syndrome region causes aortic arch defects in mice. Nature. 2001; 410:97–101. [PubMed: 11242049]
16. Bartram U, Molin DG, Wisse LJ, Mohamad A, Sanford LP, Doetschman T, Speer CP, Poelmann RE, Gittenberger-de Groot AC. Double-outlet right ventricle and overriding tricuspid valve reflect disturbances of looping, myocardialization, endocardial cushion differentiation, and apoptosis in TGF-beta(2)-knockout mice. Circulation. 2001; 103:2745–2752. [PubMed: 11390347]

Author Manuscript Author Manuscript Author Manuscript Author Manuscript

17. Choudhary B, Ito Y, Makita T, Sasaki T, Chai Y, Sucov HM. Cardiovascular malformations with normal smooth muscle differentiation in neural crest-specific type II TGFbeta receptor (Tgfbr2) mutant mice. Dev Biol. 2006; 289:420–429. [PubMed: 16332365]
18. Wu C. PINCH, N(i)ck and the ILK: network wiring at cell-matrix adhesions. Trends Cell Biol. 2005; 15:460–466. [PubMed: 16084094]
19. Hobert O, Moerman DG, Clark KA, Beckerle MC, Ruvkun G. A conserved LIM protein that affects muscular adherens junction integrity and mechanosensory function in Caenorhabditis elegans. J Cell Biol. 1999; 144:45–57. [PubMed: 9885243]
20. Clark KA, McGrail M, Beckerle MC. Analysis of PINCH function in Drosophila demonstrates its requirement in integrin-dependent cellular processes. Development. 2003; 130:2611–2621. [PubMed: 12736206]
21. Liang X, Zhou Q, Li X, Sun Y, Lu M, Dalton N, Ross J Jr, Chen J. PINCH1 plays an essential role in early murine embryonic development but is dispensable in ventricular cardiomyocytes. Mol Cell Biol. 2005; 25:3056–3062. [PubMed: 15798193]
22. Martinsen BJ, Neumann AN, Frasier AJ, Baker CV, Krull CE, Lohr JL. PINCH-1 expression during early avian embryogenesis: implications for neural crest and heart development. Dev Dyn. 2006; 235:152–162. [PubMed: 16258920]
23. Hari L, Brault V, Kleber M, Lee HY, Ille F, Leimeroth R, Paratore C, Suter U, Kemler R, Sommer L. Lineage-specific requirements of beta-catenin in neural crest development. J Cell Biol. 2002; 159:867–880. [PubMed: 12473692]
24. Soriano P. Generalized lacZ expression with the ROSA26 Cre reporter strain. Nat Genet. 1999; 21:70–71. [PubMed: 9916792]
25. Mallo M, Brandlin I. Segmental identity can change independently in the hindbrain and rhombencephalic neural crest. Dev Dyn. 1997; 210:146–156. [PubMed: 9337135]
26. Wang-Rodriguez J, Dreilinger AD, Alsharabi GM, Rearden A. The signaling adapter protein PINCH is up-regulated in the stroma of common cancers, notably at invasive edges. Cancer. 2002; 95:1387–1395. [PubMed: 12216108]
27. Murphy M, Bernard O, Reid K, Bartlett PF. Cell lines derived from mouse neural crest are representative of cells at various stages of differentiation. J Neurobiol. 1991; 22:522–535. [PubMed: 1716303]
28. Schneider JE, Bamforth SD, Farthing CR, Clarke K, Neubauer S, Bhattacharya S. Rapid identification and 3D reconstruction of complex cardiac malformations in transgenic mouse embryos using fast gradient echo sequence magnetic resonance imaging. J Mol Cell Cardiol. 2003; 35:217–222. [PubMed: 12606262]
29. Danielian PS, Echelard Y, Vassileva G, McMahon AP. A 5.5-kb enhancer is both necessary and sufficient for regulation of Wnt-1 transcription in vivo. Dev Biol. 1997; 192:300–309. [PubMed: 9441669]
30. Pietri T, Eder O, Breau MA, Topilko P, Blanche M, Brakebusch C, Fassler R, Thiery JP, Dufour S. Conditional beta1-integrin gene deletion in neural crest cells causes severe developmental alterations of the peripheral nervous system. Development. 2004; 131:3871–3883. [PubMed: 15253938]
31. Brown CB, Boyer AS, Runyan RB, Barnett JV. Antibodies to the type II TGFbeta receptor block cell activation and migration during atrioventricular cushion transformation in the heart. Dev Biol. 1996; 174:248–257. [PubMed: 8631497]
32. Loeys BL, Schwarze U, Holm T, Callewaert BL, Thomas GH, Pannu H, De Backer JF, Oswald GL, Symoens S, Manouvrier S, Roberts AE, Faravelli F, Greco MA, Pyeritz RE, Milewicz DM, Coucke PJ, Cameron DE, Braverman AC, Byers PH, De Paepe AM, Dietz HC. Aneurysm syndromes caused by mutations in the TGF-beta receptor. N Engl J Med. 2006; 355:788–798. [PubMed: 16928994]
33. Mizuguchi T, Collod-Beroud G, Akiyama T, Abifadel M, Harada N, Morisaki T, Allard D, Varret M, Claustres M, Morisaki H, Ihara M, Kinoshita A, Yoshiura K, Junien C, Kajii T, Jondeau G, Ohta T, Kishino T, Furukawa Y, Nakamura Y, Niikawa N, Boileau C, Matsumoto N. Heterozygous TGFBR2 mutations in Marfan syndrome. Nat Genet. 2004; 36:855–860. [PubMed: 15235604]

Author Manuscript Author Manuscript Author Manuscript Author Manuscript

34. Neptune ER, Frischmeyer PA, Arking DE, Myers L, Bunton TE, Gayraud B, Ramirez F, Sakai LY, Dietz HC. Dysregulation of TGF-beta activation contributes to pathogenesis in Marfan syndrome. Nat Genet. 2003; 33:407–411. [PubMed: 12598898]

Author Manuscript Author Manuscript Author Manuscript Author Manuscript

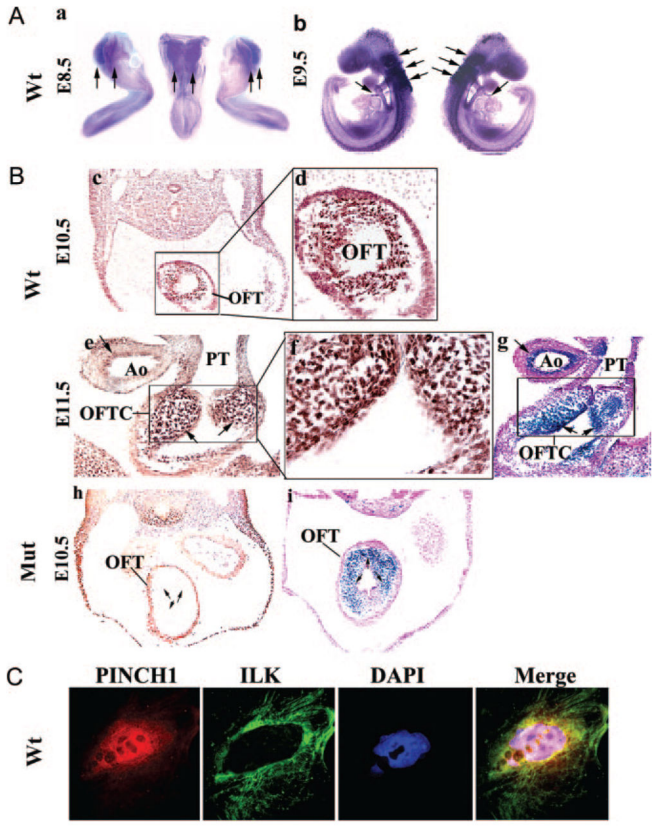

Figure 1.

Expression of Pinch1 in mouse embryos from E8.5 to E11.5. A, Whole-mount in situ hybridization analysis. Pinch1 is expressed in the cranial neural folds, including the neural folds at the level of the developing cardiac NCCs at E8.5 (a); by E9.5, Pinch1 is expressed in regions of migrating cranial and cardiac NCCs (b). Arrows indicate positive staining in regions of premigrating and migrating NCCs. B, Immunostaining with Pinch1 antibody and β-Gal staining of adjacent section from *Wnt-Cre;R26R* mice show that Pinch1 is expressed in cardiac NCCs, appearing in the outflow tract (OFT) at E10.5 (c, low magnification; d, high magnification) and outflow tract cushion (OFTC) at E11.5 (e, low magnification; f, high magnification; g, low magnification). Arrows in e indicate strong positive staining, which matches the positive β-Gal staining also pointed out by the arrows in g. PT indicates pulmonary trunk. No Pinch1 is detected in the cardiac NCCs (arrows indicate) of mutant mice at E10.5 (h). NCC fate mapping reveals the presence of NCCs (arrows indicate) in the mutant outflow tract (i). C, Immunostaining of isolated NCCs shows that Pinch1 is mainly expressed in the nucleus. ILK immunore-activity is cytoplasmic. 4′,6-Diamidino-2-phenylindole (DAPI) counterstaining indicates the nucleus. Wt indicates wild type.

Author Manuscript Author Manuscript Author Manuscript Author Manuscript

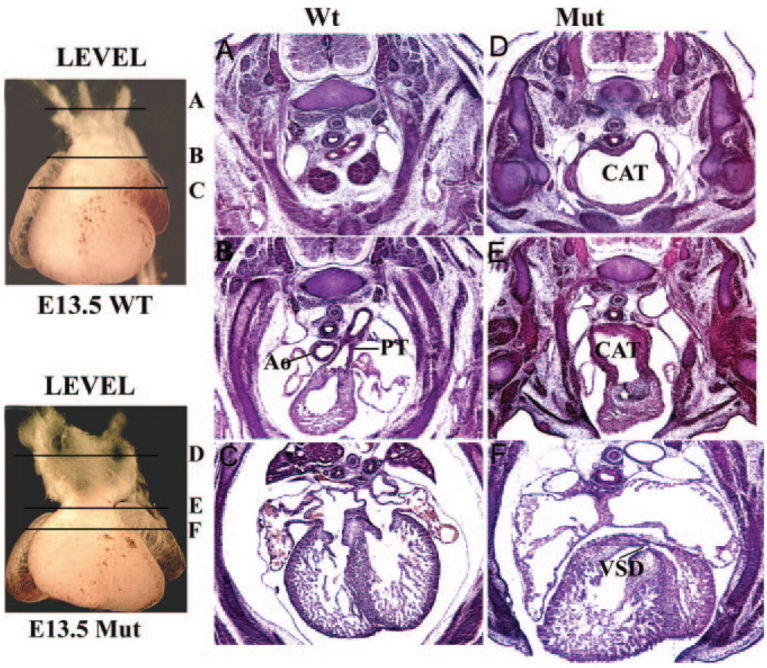

Figure 2.

Histological analysis at E13.5. A through C, Wild-type (Wt) embryos exhibit normal anatomy and structures. Pulmonary artery and the ascending aorta are separated by the conotruncal septum and right and left ventricle by the interventricular septum. Ao indicates aorta; PT, pulmonary trunk. D through F, Mutants (Mut) show dilated CAT or persistent truncus arteriosus with complete failure of outflow tract septation and VSD.

Author Manuscript Author Manuscript Author Manuscript Author Manuscript

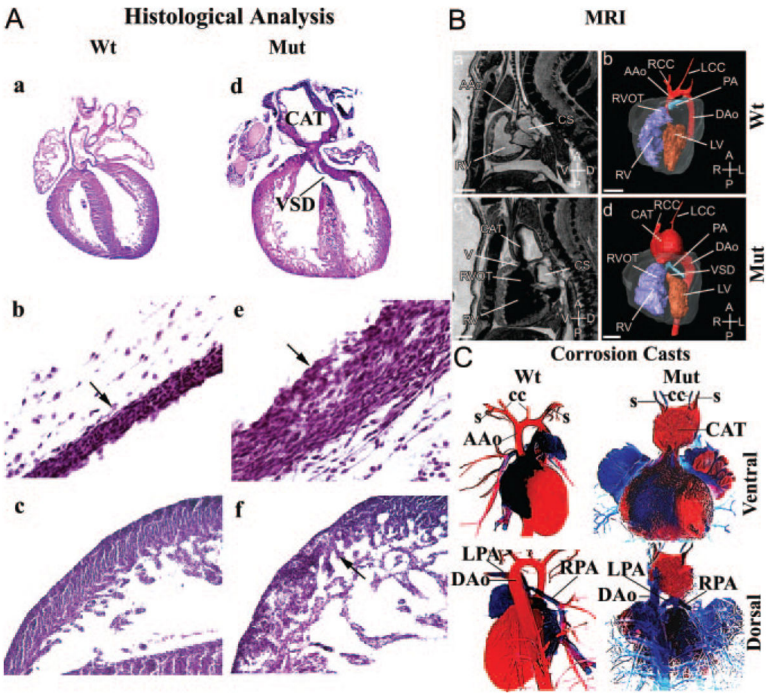

Figure 3.

Histological (A), MRI (B), and corrosion cast (C) analyses of E18.5 embryos. A, a through c, Wild-type (Wt) embryos show well-developed right and left ventricles and outflow tract: whole heart (a); wall of aorta (arrow) (b); wall of right ventricle (c). A, d through f, Mutants (Mut) exhibit enlarged CAT with a thicker wall, VSD, defective cushion-valve maturation, and enlarged heart with a thin right ventricular myocardium compact zone (arrow): enlarged heart with CAT, VSD, and defective cushion-valve maturation (d); thick wall of CAT (e); a thin right ventricular myocardium compact zone (arrow) (f). B, MRI showing sections of the thoracic viscera in *Pinch1* mutants. B, a and b, Wild-type embryo showing normal anatomy (sagittal section) and 3D reconstruction showing a ventral view. The right (RV) and left (LV) ventricles, right ventricular outflow tract (RVOT), ascending aorta (AAo), descending aorta (DAo), coronary sinus (CS), main pulmonary artery (PA), cranial arteries (CA), left CATs (LCC), and right CATs (RCC) are indicated. c and d, Corresponding section and 3D reconstruction of a Pinch1$^{-/-}$ embryo. A large VSD is present. The right ventricular outflow tract opens via a valve (V) into a CAT, which is grossly dilated and forms an aneurysmal sac. This gave rise to the aortic arch, which passes to the left of the trachea, and continues as the descending aorta. Left CATs and right CATs arose from CAT. Scale bars=500 μm; axes: d, dorsal; v, ventral; r, right; l, left; a, anterior; p, posterior. C, Corrosion casts showed that the ascending aorta gave rise to subclavian, common carotid arteries, and the right ventricle to pulmonary arteries in control embryo; CAT gave rise to subclavian, common carotid, and pulmonary arteries in mutants. CC indicates common carotid arteries; LPA, left pulmonary artery, RPA, right pulmonary artery; S, subclavian.

Author Manuscript Author Manuscript Author Manuscript Author Manuscript

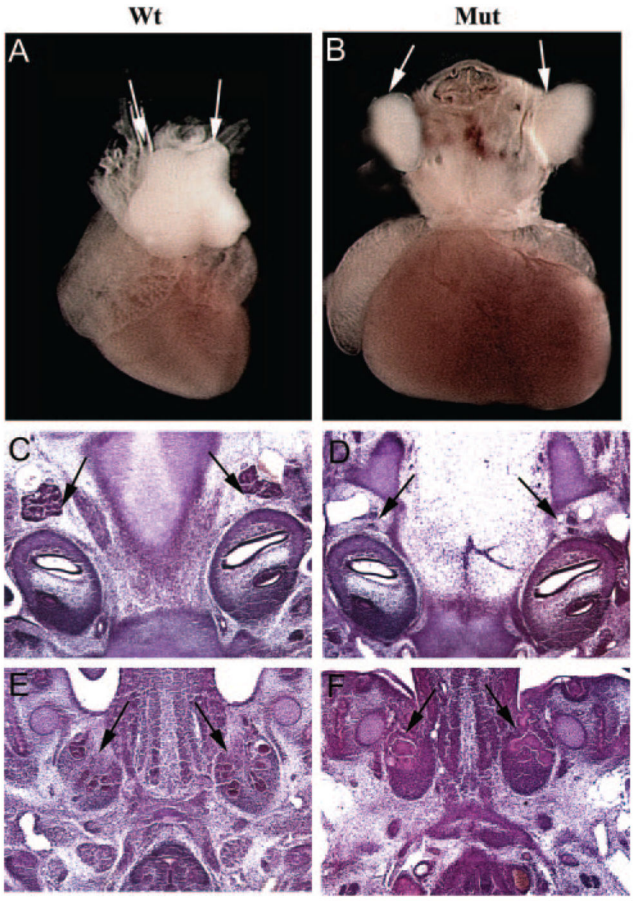

Figure 4.

Cranial neural crest–derived structure defects at E13.5. A and B, Mutant (Mut) embryos show malformed and smaller thymus (arrows) (B) compared with wild-type controls (Wt) (arrows) (A). C through F, Histological analysis on transverse sections of the head at E13.5 show smaller or absent glossopharyngeal ganglia (IX) (arrows) (D), and disrupted submandibular glands (arrows) (F) in mutant embryos compared with controls (arrows) (C and E).

Author Manuscript Author Manuscript Author Manuscript Author Manuscript

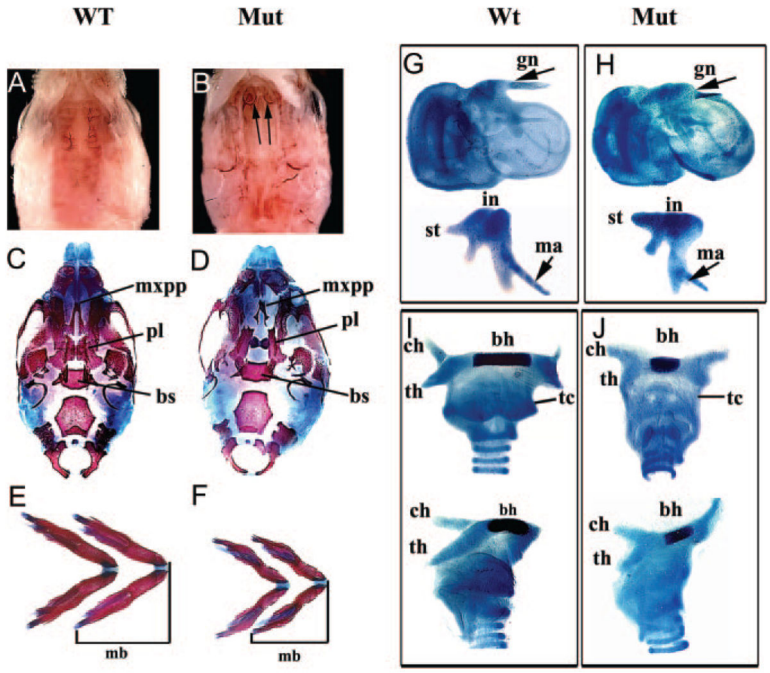

Figure 5.

Cranial neural crest–derived structure defects at E18.5. Mutant (Mut) embryos show a cleft palate (arrows) (B) compared with wild-type controls (Wt), which have normal palate closure (A). C through J, Hypoplastic or malformed structures of bone and cartilage in the head and neck of mutant embryos. Ventral views of skull skeletal preparations in which mandible was removed for visualization of the palate (C and D). Shown are mandible bones (E and F), otic capsules with associated elements, and the neck structures (hyoid and laryngeal cartilages) (G through J). ch indicates ceratohyoid; gn, gonial; in, incus; ma, malleus; mb, mandibular bone; mxpp, palatal process of maxilla; pl, palatine; st, stapes; tc, thyroid cartilage; th, thyrohyoid.

Author Manuscript Author Manuscript Author Manuscript Author Manuscript

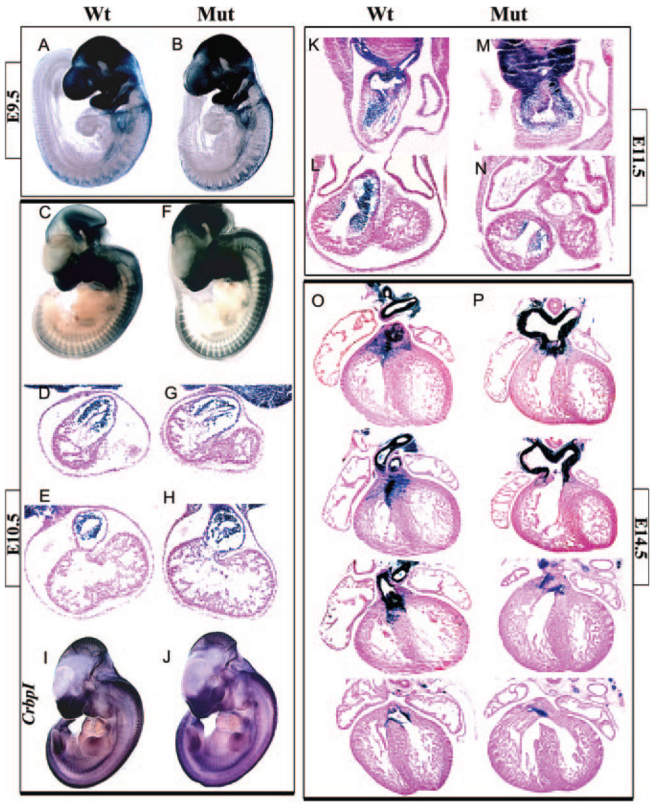

Figure 6.

Fate mapping and in situ hybridization analysis of NCC migration in wild-type (Wt) and mutant (Mut) E9.5 to E14.5 embryos. A through H, Fate-mapping analysis in E9.5 (A and B) and E10.5 (C through H) embryos. NCCs migrated into the cranial region, pharyngeal arches, and trunk region of both E9.5 wild-type (A) and mutant (B) embryos. NCCs are observed in the cranial region and pharyngeal arches as well as in the lateral walls of the aortic sac and outflow tract in both mutants (F through H) and control littermates (C through E). I and J, Whole-mount in situ hybridization using the *Crbp1* probe shows NCCs in the cranial region, pharyngeal arches, and trunk region around E10.5 through E11.0 in wild-type (I) and mutant (J) mice. K through P, Fate-mapping analysis at E11.5 (K through N) and E 14.5 (O and P). NCCs contribute to formation of the outflow septum and outflow cushions of wild-type embryos (K, L, and O); in mutants, NCCs densely gather in the persistent conotruncal region and positively stained cells in the proximal region of outflow cushions and valves are absent or greatly reduced (M, N, and P).

Author Manuscript Author Manuscript Author Manuscript Author Manuscript

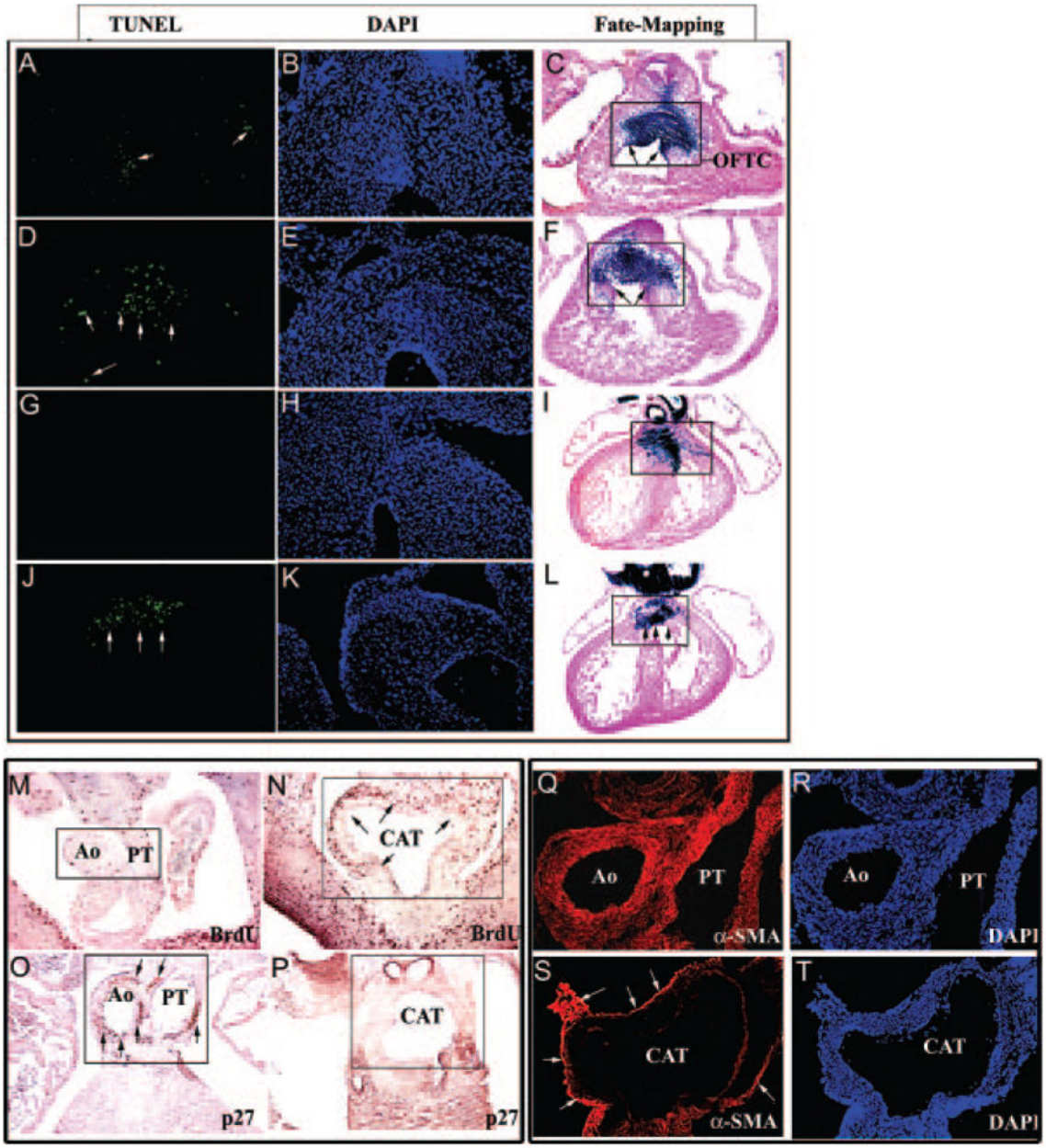

Figure 7. TUNEL staining, BrdUrd labeling, and differentiation assays

A through L, TUNEL staining was performed on sections from E11.5 (A through F) and E 13.5 (G through L) embryos. A few TUNEL-positive cells are observed in the cushion of wild-type control embryos (arrows) (A) but are not seen in the membranous septum (G). Markedly increased apoptosis is observed in the cushion and membranous septum (arrows) (D and J) of mutant embryos. The regions in A, D, G, and J correspond with the boxed areas of adjacent sections stained with β-Gal in C, F, I, and L (arrows indicate the regions where apoptosis occurs), respectively. M and N, BrdUrd labeling reveals increased BrdUrd incorporation in the out-flow region of mutants at E11.5 (shown in the box with arrows) (N) compared with control embryos (shown in the box) (M). O through T, Differentiation

Author Manuscript Author Manuscript Author Manuscript Author Manuscript

analysis using p27 (O and P) and α-SMA (Q and S) antibodies with 4′,6-diamidino-2-phenylindole (DAPI) counterstaining (R and T) show that cells positive for p27 and α-SMA are present in the out-flow tract of wild-type embryos at E11.5 (O, arrows, and Q), respectively, whereas signals positive for p27 and α-SMA are reduced or absent in mutants at E11.5 (P and S). Note that expression of α-SMA in mutant pharyngeal arch arteries and out layer of the outflow tract is relatively unaffected (arrows) (S). Ao indicates aorta; PT, pulmonary trunk.

Author Manuscript Author Manuscript Author Manuscript Author Manuscript

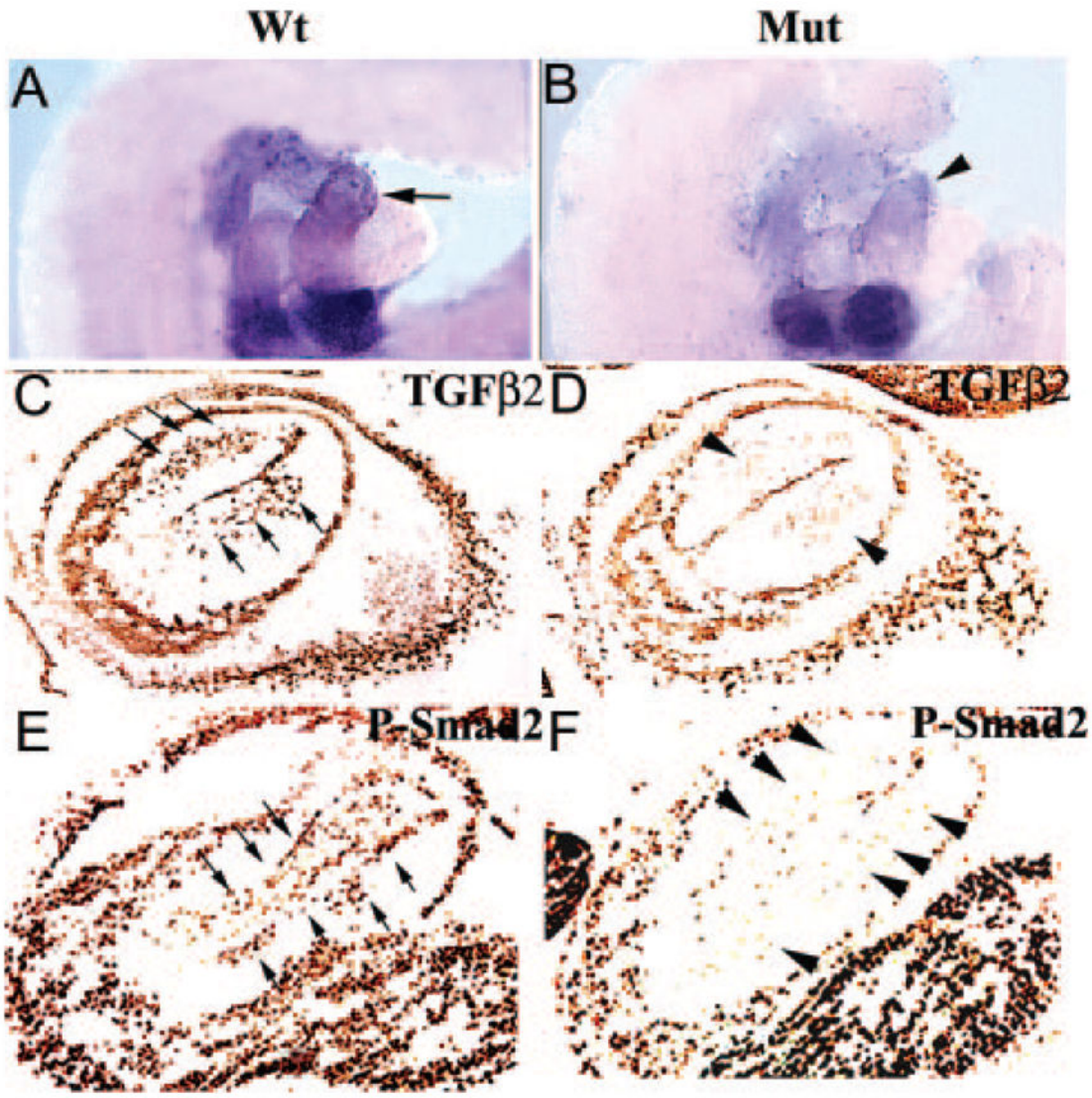

Figure 8.

Analysis of TGFβ_2 signaling in wild-type (Wt) littermates and Pinch1 mutants (Mut) at E10.5. A and B, Whole-mount in situ hybridization shows a reduction of TGFβ_2 expression in the outflow tract of mutants (arrowhead) (B) compared with controls (arrow) (A). C and D, Immunostaining with a TGFβ_2 antibody shows that TGFβ_2-positive cells are observed in the outflow tract of wild-type embryos (arrows) (C), a reduction or absence of TGFβ_2-positive cells is observed in the outflow tract of mutants (arrowheads) (D). E and F, Immunostaining with a P-Smad2 antibody shows a reduction or absence of P-Smad2–positive cells in the outflow tract of mutants (arrowheads) (F) compared with controls (arrows) (E).